Applied Catalysis B: Environmental 179 (2015) 276–284

Contents lists available at ScienceDirect

Applied Catalysis B: Environmental

journal homepage: www.elsevier.com/locate/apcatb

Electrochemical reforming of alcohols on nanostructured platinum-tin catalyst-electrodes

A.R. de la Osa [a], A.B. Calcerrada [a], J.L. Valverde [a], E.A. Baranova [b], A. de Lucas-Consuegra [a,*]

[a] Departamento de Ingeniería Química, Facultad de Ciencias y Tecnologías Químicas, Universidad de Castilla-La Mancha, Avenida Camilo José Cela 12, 13005 Ciudad Real, Spain

[b] Department of Chemical and Biological Engineering, Center for Catalysis Research and Innovation (CCRI) University of Ottawa, 161 Louis-Pasteur St., Ottawa ON K1N 6N5, Canada

ARTICLE INFO

Article history:
Received 2 February 2015
Received in revised form 7 May 2015
Accepted 12 May 2015
Available online 19 May 2015

Keywords:
Electrochemical reforming
H_2 production
Ethanol electrolysis
PEM
Pt–Sn catalysts

ABSTRACT

This study reports the feasibility of high purity H_2 production by means of the electrochemical reforming of biomass derived organic alcohols (methanol, ethanol and ethylene glycol)-water solutions in a proton exchange membrane (PEM) electrolysis cell. For that purpose, a nanostructured bimetallic carbon-supported Pt–Sn catalyst, with nominal Pt/Sn atomic ratios of 70/30, was synthesized by a modified polyol reduction method and characterized by means of TEM, XRD and XPS analysis. The resulting Pt_7–Sn_3/C catalyst consists of a bi-phase Pt/SnO_x structure and presents a narrow particle size distribution with size predominantly in the order of 4.5 nm, showing high dispersion on carbon support (20 wt.% metal loading). During electrochemical reforming tests, the influence of reaction temperature and the electrocatalytic stability of the system were verified for mild working operation times. Synthesized 20 wt.% Pt_7–Sn_3/C anodic catalyst provided a promising electro-catalytic activity, comparable to that of commercial 60 wt.% Pt–Ru/C and required lower amounts of Pt in order to produce the same amount of hydrogen. Proposed system allowed to produce H_2 with a lower electrical energy requirement (26 kWh $kg_{H_2}^{-1}$ even after deactivation), in comparison with commercial PEM water electrolyser stacks (50 kWh $kg_{H_2}^{-1}$). In addition, obtained H_2 purity was very high (99.938%) and only few ppm of CO and CO_2 were detected at the cathode chamber. These results demonstrated the potential interest of Pt_7–Sn_3/C anodic catalyst, synthesized via the polyol method, for production of pure hydrogen from biomass-derived compounds via electrochemical reforming at low temperatures.

1. Introduction

Hydrogen has attracted great interest as a future clean fuel for combustion engines and fuel cells [1]. It can be obtained by different processes and from a wide variety of materials (water, biomass, or hydrocarbons). Among them, the catalytic steam reforming of methane is currently being the most used in industry. However, this process required several reaction steps, such as reforming, water gas-shift and preferential oxidation (PROX) or methanation, in order to clean the reformer gas stream from CO before entering the fuel cell. Therefore, due to its practical use, especially for on-site applications, more efficient and compact processes for hydrogen production should be considered [2]. Electrolysis of water can generate highly pure hydrogen, in a fast single step process, and hence it can be considered as the most promising technology for small scale H_2 production [3]. The drawback of this process is the high-energy requirement. Theoretically, an energy consumption of 39.4 kWh kg^{-1} or 3.54 kWh/Nm^3 is required for the production of H_2. However, commercial electrolyzes require up to 50–55 kWh kg^{-1} or 4.5–5 kWh/Nm^3 [4]. In the last years, the electrolysis of alcohols (also called Electrochemical Reforming) have shown to be a promising method to decrease the energy demand ascribed to the electrolytic production of hydrogen [5]. An electrochemical reformer may operate in a similar way to a proton exchange membrane (PEM) water electrolysis cell. However, instead of water, an aqueous solution of the organic compound is electro-oxidized at the anodic side leading to the formation of other organic compounds, protons and electrons. The external circuit provides the electrical potential to drive the reaction, while protons migrate through the proton exchange membrane to the cathode side, where they recombine with electrons, which have passed through the external circuit to form pure hydrogen gas. In

* Corresponding author. Tel.: +34 926295300; fax: +34 926 295437.
E-mail address: Antonio.lconsuegra@uclm.es (A. de Lucas-Consuegra).

http://dx.doi.org/10.1016/j.apcatb.2015.05.026
0926-3373/

Table 1
Advantages and drawbacks of electrochemical reforming vs. catalytic steam reforming.

	Electrochemical reforming of alcohols	Catalytic steam reforming
Advantages	• Lower reaction temperatures (<100 °C) making possible a rapid startup • Low toxicity • Direct pure hydrogen production, separated from other reaction products • Easier and fast control of hydrogen production rate • Compact unit combining both reaction and hydrogen purification with a consequent capital costs reduction • High renewable energy integration • Reduced environmental impact • Seasonal energy storage without energy losses • Capability to handle power fluctuations by H_2 production • Lower power demands than water electrolysis, since part of the energy required is provided by the organic molecule	• Mature technology • Adequate legislature framework • Practical experience in plant operations • Safety of power and energy supply
Drawbacks	• Immature technology • Limited practical experience • Required development of more active catalysts and more stable membranes • High cost anodic catalyst typically based on Pt–Ru/C	• Higher reaction temperatures (200–1000 °C) • Poor hydrogen purity by production of H_2/CO mixtures, CO_2 and CH_4 • Required purification stages (multistep process) affecting negatively the overall process in terms of costs and efficiency • Pollutant emissions • Application of non-renewable resources • Catalyst deactivation due to coking

this context, recent studies have shown that the electrochemical reforming of water–alcohol mixtures, i.e., methanol [5–8], glycerol [9,10], ethanol [11,12], bioethanol [13,14] and ethylene glycol [15] has a great potential for H_2 production at atmospheric pressure. The use of such compounds allows electrolysis at potentials lower than 1.2 V, leading to electrical power savings if compared to conventional electrolytic water splitting. Table 1 also summarizes some interesting advantages of electrochemical reforming of alcohols vs. their catalytic conversion for H_2 production. In addition, similar energy requirements can be found for electrochemical reforming of alcohols (149–193 kJ/mol H_2, this work) compared to those obtained in a thermodynamic study of conventional steam reforming of ethanol (100–260 kJ/mol H_2 for 1000–400 °C) [16].

While undoubtedly promising, the electrochemical reforming approach suffers the limitation of delivering low current densities that must be improved for the technological exploitation of this kind of systems. Pt is known to be the best active and stable noble metal for alcohol oxidation, particularly in acid media [17]. However, the limitation of the usage of Pt-based catalysts comes from its high cost, limited resources and tendency for surface poisoning that could be mitigated by adding a second metal. Hence, the use of a bimetallic catalyst involving the addition of Ru, Sn, Os among others, has been reported to promote alcohol electro-oxidation in both acid an basic media [18–25]. Pt–Sn nanocomposites have been extensively studied as catalysts for the electro-oxidation of hydrogen/carbon monoxide, methanol and ethanol for electricity production in PEM fuel cells. A good CO tolerance during H_2 oxidation has been proved but regarding the methanol or ethanol electro-oxidation, controversial results depending on the phase of Sn [26] and Pt/Sn atomic ratio [23,27] have been described. Furthermore, alcohol oxidation reactions are well known to be structure sensitive, therefore particle size, dispersion, morphology and agglomeration degree, as well as surface and bulk structure, which strongly depends on the preparation method, have to be considered [23,28]. It is established that the electrocatalyst performance depends substantially on the atomic ratios of elements present, and the optimal composition of Pt–Sn/C for ethanol oxidation varies depending on the synthesis procedure and the reaction conditions. Lamy et al. [27] studied Pt/Sn compositions ranging from 4/1 to 9/1 and found that the addition of Sn always promoted the ethanol electro-oxidation compared to Pt. Even more, the presence of 10–20 at.% Sn resulted in the best resistance to catalyst poisoning or deactivation. Zhou et al. [29] published that the Pt–Sn composition of 33–40 at.% Sn provides the best ethanol electro-oxidation current densities for fuel cell applications. Recently, carbon supported Pt–Sn/C electro-catalysts with 30 at.% Sn (Pt_7–Sn_3/C), synthesized by the modified polyol method, were reported to have high catalytic activity for ethanol electro-oxidation in acid [30] and alkaline [31] solutions. According to the latter studies, the aim and contribution of the present work was to evaluate for the first time the application of these Pt_7–Sn_3/C nanoparticles with average particle size of 4.5 nm to the electrochemical reforming of ethanol, ethylene glycol and methanol for pure H_2 production in a PEM membrane fuel cell type reactor. In addition, a mild term stability study was developed in order to evaluate the real energy requirements of produced H_2, and hence, the practical feasibility of the proposed catalytic system, in comparison with a commercial PEM water electrolyzer.

2. Experimental

2.1. Preparation of the carbon-supported Pt_7–Sn_3/C catalyst

Colloidal Pt–Sn nanoparticles were synthesized using modified polyol reduction method [32,33], using ethylene glycol (EG) as a stabilizing and reducing agent. EG also acted as a surfactant after precursor metal salt reduction, preventing any particle agglomeration after the formation of colloidal particles. The detailed synthesis procedure of Pt–Sn nanoparticles with the atomic ratio of Pt to Sn of 70/30 at.% is described in details elsewhere [30]. In short: 19.8 mg of tin (II) chloride anhydrous (ACROS Organics, 98% Anhydrous) and 82.2 mg platinum (IV) chloride (Alfa Aesar, 99.9% metal basis, Pt (57.75%)) were used as precursors. First, those salts were dissolved in 50 mL of EG (anhydrous 99.8% Sigma-Aldrich) containing 0.2 M of NaOH (EM Science, ACS grade), pH 11. The solution was stirred for 1 hour at room temperature and then refluxed at 190 °C for 2 h. The dark brown colloidal solution containing Pt_7–Sn_3 nanoparticles (concentration of colloids in EG is 1.2 mg/mL) was cooled down to room temperature. The colloidal solution was then dispersed on a carbon support (Vulcan XC 72, Cabot) by mixing in a large beaker an appropriate amount of colloidal solution and carbon for up to 24 h, resulting in 20 wt.% metal loading. Carbon-supported Pt_7–Sn_3 catalyst was extensively washed with DI water (18 MΩ cm) and then

dried in air at 80 °C for 3 h. No further pre-treatment was performed to the catalyst.

2.2. Catalyst characterization

X-ray diffraction powder patterns were run using a Bruker AXS D8 Advance system powder diffractometer, equipped with a Cu tube and a Vantec position-sensitive detector with radial Soller slits to reduce the background at low angles. Diffractograms were collected between 30° and 100° 2θ with a very small step of 0.0142° 2θ and by accumulating data for 60s per step.

Size and morphology of the nanocatalyst was also investigated by transmission electron microscopy (TEM). TEM analysis of carbon-supported Pt_7–Sn_3/C catalyst was carried out using a JEOL JEM 2100F FETEM microscope operating at 200 kV. Carbon-supported Pt_7–Sn_3 nanoparticles were suspended in ethanol. A drop of catalyst suspension was applied directly onto clean copper grids and dried in the oven at 80 °C for 2 h. The sample was then pumped for 24 h using the turbo-pump (Varian V-81 M Turbo Station) to remove any presence of gases and dust from the sample holder. Determination of Pt_7–Sn_3/C particles size distribution was carried out using Image J software by measuring at least 300 nanoparticles from the TEM images.

Carbon-supported Pt_7–Sn_3 catalyst was analyzed by Kratos Axis Ultra DLD X-ray Photoelectron Spectrometer. XPS analysis was conducted at 140 W at pass energy of 20 eV. Peak positions were corrected for sample charging by setting the maximum of C 1s peak to binding energy of 284.7 eV. Data analysis and quantification were performed using CasaXPS software. A linear background subtraction was used for quantification of C 1s and O 1s and Shirley for Pt 4f and Sn 3d spectra. Sensitivity factors provided by the manufacturer were utilized. 70% Gaussian/30% Lorentzian line shape was used in the curve-fit. For species identification, Pt 4f spectra have been deconvoluted based on the constraints of equal spin-orbit splitting of 3.4 eV. FWHM was used based on that for Pt 4f spectrum from Pt foil [34].

2.3. Preparation of membrane electrode assembly (MEA)

Synthesized bimetallic Pt–Sn (70/30 at.% Pt/Sn) nanoparticles supported on carbon (20 wt.%) were used as anode, while Pt supported on carbon (20 wt.% Pt/C-Alfa Aesar) was adopted as cathode. Catalyst inks were prepared by mixing appropriate amounts of the catalyst powders with Nafion solution (5 wt.%, Sigma–Aldrich) and isopropanol with a binder/solvent volume ratio of 0.04. Inks were deposited on Carbon Paper (Fuel Cell Earth) substrates of 6.25 cm^2 geometric area until, after drying, a metal loading of 1.5 mg/cm^2 for the anode and 0.5 mg/cm^2 for the cathode were obtained. The electrolyte consisted of a proton conducting Sterion® membrane of 185 μm thickness (supplied by Hydrogen Works). Prior to use, the polymeric membrane was pretreated by successive immersion at 100 °C for 2 h in H_2O_2 and H_2SO_4 solutions and deionized water. MEA was then prepared with hot pressing, under 1 metric ton at 120 °C for 3 min.

2.4. Electrochemical reforming activity measurements

Experimental tests were carried out in a PEM electrolysis cell. The MEA was fastened between two Teflon gaskets, appropriately designed, with two purposes: (i) to ensure sealing between anode and cathode compartments and, (ii) to avoid short-circuiting of the cell. Graphitic bipolar plates of 2 cm thickness and 36 cm^2 area were placed on both sides of the MEA. Plates hosted parallel grooves, with a total surface area of 6.25 cm^2, which served as flow channels. Except from providing reactants and products distribution, the bipolar plates also served as current collectors. All the above items were finally placed between two external Teflon plates covered with metallic end plates (1 cm thickness and 100 cm^2 area). Then, they were uniformly tight with nuts and bolts using an electronic torque wrench in order to ensure mechanical stability. The cell had provisions for heating and temperature control and was equipped with ports for the supply of the reactants and the removal of the products.

Electrochemical measurements were carried out in the experimental setup explained in detail elsewhere [11] with an Autolab potentiostat/galvanostat (PGSTAT30-ECOCHEMIE) controlled by a Research Electrochemistry software. Anode compartment of the cell was fed with 6 M alcohol–water solutions (1 L) at 60 ml h^{-1}, using a high-pressure liquid pump (HPLP-GILSOM 307). Fuel concentration was selected according to previous works, where this value was found to be the optimal for Pt–Ru/C anodic catalyst [11,13]. Cathode chamber was supplied with water, by a syringe pump at a constant 10 ml h^{-1} flow rate, in order to keep a suitable humidity on the membrane. Both feeding solutions were preheated at a temperature close to that of the cell, which was always kept in a temperature range between 60 and 90 °C. Data results were obtained with gradual polarization from 0.4 V to a maximum applied potential of 1.1 V. Reaction products (outlets of anode and cathode compartments) were passed through a cooling condensation column (−6 °C) to separate liquid and gas phase species. Analysis of the liquid anodic and gaseous cathodic products were carried out using a double channel gas chromatograph (Bruker 450-GC). It is equipped with: (a) thermal conductivity detector connected to a Hayesep (Q 80/100 mesh UM 1.5 m 1/16 inch diameter) and a Molsieve (13X UM 1.2 m 1/16 inch diameter) consecutive columns; (b) flame ionization detector connected to a CP-Wax 52CB column of 25 m × 0.53 mm × 2 μm, CP7658, using Ar as carrier gas. For the analysis of the anodic chamber stream, the solution was recycled for 10 h in order to achieve quantified amount of products. In addition, during the electrochemical reforming experiments, hydrogen production rate was also followed by gas–volume measurements and crosschecked via Faraday's Law calculations, based on the cell current.

3. Results and discussion

3.1. Catalyst characterization

Synthesized catalyst was characterized by means of TEM, XRD, and XPS methods as described above. Fig. 1 shows XRD patterns of

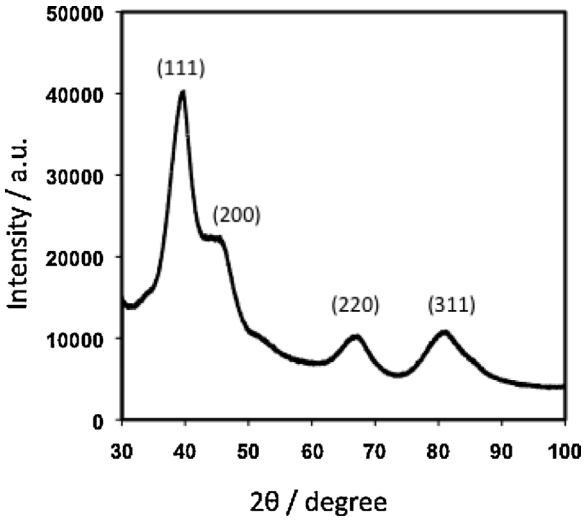

Fig. 1. XRD pattern of Pt_7–Sn_3/C anodic catalyst.

Table 2
XPS data of Pt_7–Sn_3/C catalyst.

Pt4f		
Species	Binding energy (eV)	at. (%)
Pt	71.6	38.6
PtO	72.3	30.5
$Pt(OH)_2$	73.1	17.9
PtO_2	74.2	13.0
Sn 3d		
Sn	485.9	9.0
SnO_x	487.4	91.0

Pt_7–Sn_3/C catalyst. It can be seen that the structure of nanoparticles was face-centered cubic (fcc) typical for bulk and nano-structured Pt [35,36]. Peaks around 40, 46, 68 and 81° 2θ corresponded to Pt fcc reflections (1 1 1), (2 0 0), (2 2 0) and (3 1 1), respectively. There was no separate SnO_2 crystalline-phase observed for Pt_7–Sn_3/C sample. As reported earlier [30], for Pt–Sn prepared at high sodium hydroxide concentrations (C_{NaOH} = 0.2 M, initial pH 11), only partial alloying between Pt and Sn occurred and nanoparticles with a structure and composition close to that of pure Pt were formed. No evidence of metallic Sn or SnO_2 crystalline phases were found on XRD patterns, suggesting that tin is present in an amorphous state. Therefore, Pt_7–Sn_3/C catalyst presented bi-phase Pt/SnO_x structure. Crystallite size of the catalyst was calculated using the (2 2 0) reflection according to Debye formula for scattering by randomly oriented molecules, as reported earlier for colloidal Pt and Pt_xRu_{1-x}, [35] as well as for carbon-supported Pt–Sn catalysts [30]. This reflection was selected for the calculation of the crystallite size because carbon Vulcan XC-72 support has strong graphite peaks near 25 and 45° 2θ, due to 0 0 2 and 1 0 1 reflections, respectively. The presence of these two peaks that overlap with the main fcc (1 1 1) and (2 0 0) diffraction peaks prevents an accurate crystallite size evaluation. Crystallite size of Pt_7–Sn_3/C nanoparticles was found to be 3 nm.

Typical TEM micrographs of Pt_7–Sn_3/C catalyst are shown in Fig. 2. It can be seen that resulting nanoparticles are spherical in shape over a narrow particle size distribution (Fig. 2c). Average particle size of Pt_7–Sn_3/C was 4.5 nm, demonstrating that the selected method was adequate for the preparation of nanomaterials with well-defined size.

Furthermore, as detailed elsewhere [34,37] and depicted in Table 2, curve-fitting of the high resolution XPS spectra of Pt 4f and Sn 3d core level peaks (not shown here) revealed the presence of platinum in Pt, PtO, $Pt(OH)_2$, PtO_2 and tin in Sn and SnO_x in Pt_7–Sn_3/C catalyst. Presence of PtO_x on the catalyst surface is related to the synthesis method of nanoparticles. Colloidal nanoparticles are synthesized in ethylene glycol in a round bottom flask, which is open to the air. Catalysts are used as prepared without any pre-treatment or reduction in H_2. Binding energies for SnO_2 and SnO were quite similar, so it was difficult to distinguish between these two species, however XPS was able to confirm that the main part of Sn was in the oxidized state [30].

3.2. Electrochemical reforming experiments for H_2 production

In order to preliminary test the electrochemical reforming behavior of catalyst Pt_7Sn_3/C, a linear voltammetry was performed at a fixed temperature of 80 °C using 6 M ethanol solution as fuel to the anode. Fig. 3 shows that, as expected, an increase in the applied potential leads to higher currents densities and consequently, higher production rates of H_2. Moreover, it can be observed that obtained current is completely related to hydrogen produced in the cathodic side of the PEM configuration by the Faraday law. The perfect fit between experimental measurements of gas-volumetric

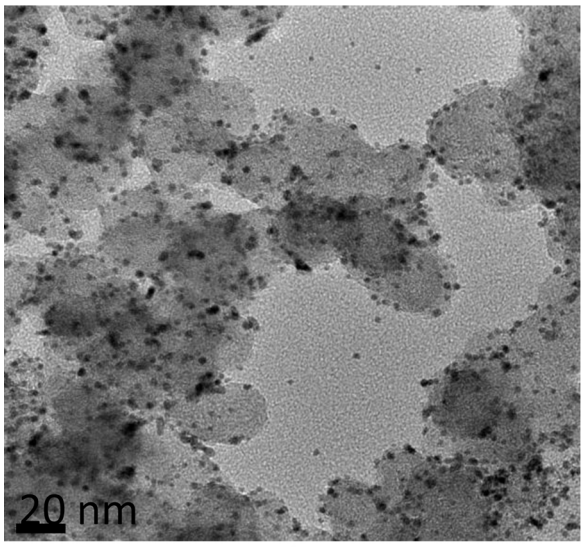

a)

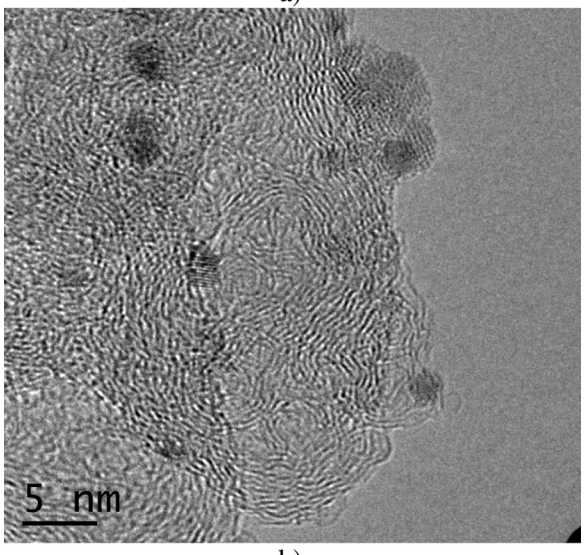

b)

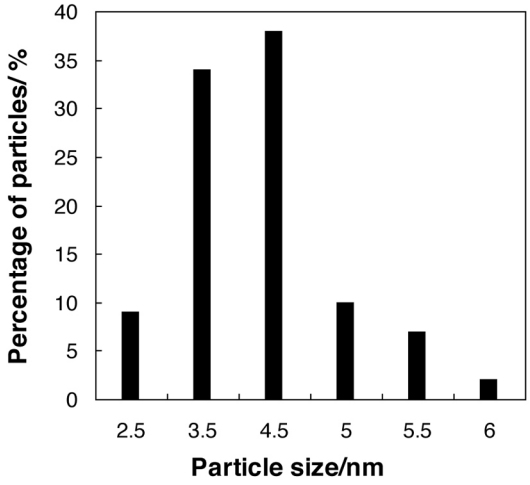

c)

Fig. 2. TEM images (a), high resolution TEM (b) and corresponding histograms (c) of the carbon supported Pt_7–Sn_3/C catalyst.

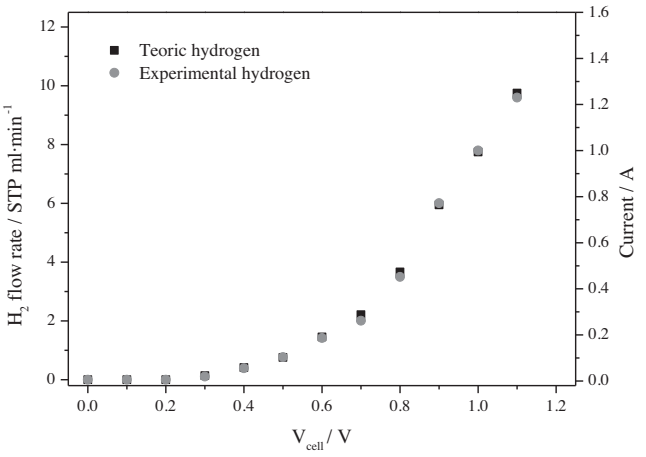

Fig. 3. Influence of the applied potential on the obtained current and the experimental and theoretical H_2 production rates using 6 M ethanol/water solution at 80 °C.

H_2 flow and those predicted by Faraday's Law demonstrated that practically 100% of the applied electrical energy was used for H_2 production.

Once the viability of the proposed system was proved, an analysis of reaction temperature has been accomplished. Fig. 4 depicts the variation of the steady-state current density and the corresponding hydrogen production rate with the applied potential for methanol–water, ethanol–water and ethylene glycol–water solutions at 60 °C, 70 °C, 80 °C and 90 °C, respectively. The same trend explained above was observed for the entire explored reforming temperature range. It is worthy to note that hydrogen production is only attributed to the electro-oxidation of the organic compounds, since no current was obtained in the whole potential range (0–1.1 V) by feeding pure deionized water (as verified in separate experiments, not shown here). The increase of hydrogen production rate by rising the applied potential can be attributed to the enhanced kinetics of electrochemical reactions. On the other hand, the shape of the obtained curves indicates that the performance of the cell was mostly dictated by activation and ohmic losses, since no limiting current was obtained in the potential range of interest [11,13]. It can be observed that hydrogen production started at potentials above 0.4 V independently on the three investigated temperatures or feedstocks. A similar onset potential of 0.4 V was found in previous studies of electrochemical reforming for each molecule: ethanol [11], methanol [6] and ethylene glycol [15] with commercial Pt–Ru/C anodic catalyst of larger metal loading (60 wt.%) for similar aqueous organic concentrations (1–6 M). Moreover, in all cases, an increase of reaction temperature led to an increase of current, enhancing therefore hydrogen production rate at the cathode of the electrochemical cell. It can be attributed to both the increase of ionic conductivity of the membrane at fixed potential and the enhancement of kinetics of electrochemical reforming reactions with the working temperature [11]. It is also interesting to note that although slight differences were found at 60 °C among the fuels, methanol solution showed the highest electro-catalytic activity compared to the other molecules at fixed temperature and potential. Complete oxidation of ethanol and ethylene glycol to CO_2 was more difficult than that of methanol (a single carbon molecule) due to the difficulties in C—C bond breaking and the formation of CO-intermediates that poisoned platinum anode catalyst [38–40]. Ideal reaction pathways take place as follows:

(a) Methanol electroreforming [7]:

$$\text{Anode}: CH_3OH + H_2O \rightarrow CO_2 + 6H^+ + 6e^- \quad (1)$$

$$\text{Cathode}: 3\cdot(2H^+ + 2e^- \rightarrow H_2) \quad (2)$$

$$\text{Overall}: CH_3OH + H_2O \rightarrow CO_2 + 3H_2 \quad (3)$$

(b) Ethanol electroreforming [41]:

$$\text{Anode}: CH_3CH_2OH \rightarrow CH_3CHO + 2H^+ + 2e^- \quad (4)$$

$$\text{Cathode}: 2H^+ + 2e^- \rightarrow H_2 \quad (5)$$

$$\text{Overall}: CH_3CH_2OH \rightarrow CH_3CHO + H_2 \quad (6)$$

(c) Ethylene glycol electroreforming [42]:

$$\text{Anode}: C_2H_6O_2 + H_2O \rightarrow C_2H_4O_3 + 4H^+ + 4e^- \quad (7)$$

$$\text{Cathode}: 2\cdot(2H^+ + 2e^- \rightarrow H_2) \quad (8)$$

$$\text{Overall}: C_2H_6O_2 + H_2O \rightarrow C_2H_4O_3 + 4H_2 \quad (9)$$

However, at temperatures over 70 °C, obtained results seemed to be comparable to those for ethanol and ethylene glycol over commercial bimetallic 60 wt.% Pt–Ru/C anodic catalyst reported elsewhere [11,15]. It appeared that, as in methanol oxidation on a Pt–Ru, two effects are involved in ethanol and ethylene glycol electro-oxidation on Pt_7–Sn_3/C, i.e., the bifunctional mechanism and the ligand effect [20,43]. The presence of tin also allowed ethanol/ethylene glycol to adsorb dissociatively and then to break the C—C bond, resulting in small amounts (ppm) of CO or CO_2 as will be shown later in Table 4. Moreover, it has been reported earlier [23,44] that tin oxide provides oxygen-containing species at lower potential than platinum. Oxygen-containing species, whose amount depends on Sn oxidation state, Pt/Sn surface ratio and structure, may react with CO-like poisonous intermediates of ethanol electro-oxidation. As seen from the obtained results, synthesized Pt_7–Sn_3/C catalyst showed high catalytic activity for EG and ethanol oxidation by supplying sufficient $-OH_{ads}$ and Pt active sites, as well as having aceptable ohmic effect. Hence, it can be considered as an appropriate anode for both EG and ethanol electroreforming. It can also be observed that ethylene glycol/water solution displays a slightly higher electrocatalytic activity compared to that of the ethanol/water mixture. It may be attributed to the fact that EG molecule presents two OH^- groups available, which are found to have a preference for the Sn sites [45].

Fig. 5a and b summarizes electro-reforming energy requirements related to each alcohol/water solution at the established temperature range (70–90 °C) and at fixed current of 0.5 A (0.08 A cm^{-2}) or 1.2 A (0.192 A cm^{-2}), respectively. Results at 60 °C are not shown since the comparison was only possible at the lowest current density (see Fig. 4). In agreement with polarization curves, the electrical energy required to generate a certain amount of hydrogen decreases at higher reaction temperatures. Indeed, electricity consumption was reduced from 10 to 15% for the three explored molecules by increasing reaction temperature from 70 to 90 °C, which is due to favored kinetics and membrane ionic conductivity, as mentioned above. However, it is clear that a higher amount of heat (thermal energy) should be supplied to the PEM cell at higher temperatures. A previous work of electrochemical reforming of ethylene glycol on Pt–Ru/C anodic catalyst [15] reported a complete energy analysis, including all different units comprised in the electrochemical reforming process (pumps, heaters, electrical energy, etc.). Electrical energy consumption of the electrochemical reforming unit (alcohol electrolysis) resulted to be the main energy requirement of the whole process compared to other operational energy demands. Then, the authors reported the highest explored temperature (90 °C) and low current densities (0.08 A cm^{-2}) as optimal conditions for the minimization of H_2 production energy. Accordingly, an increase of current density led to an increase of the electrical energy requirement for the electrochemical reforming of each molecule. However, other parameters should be considered

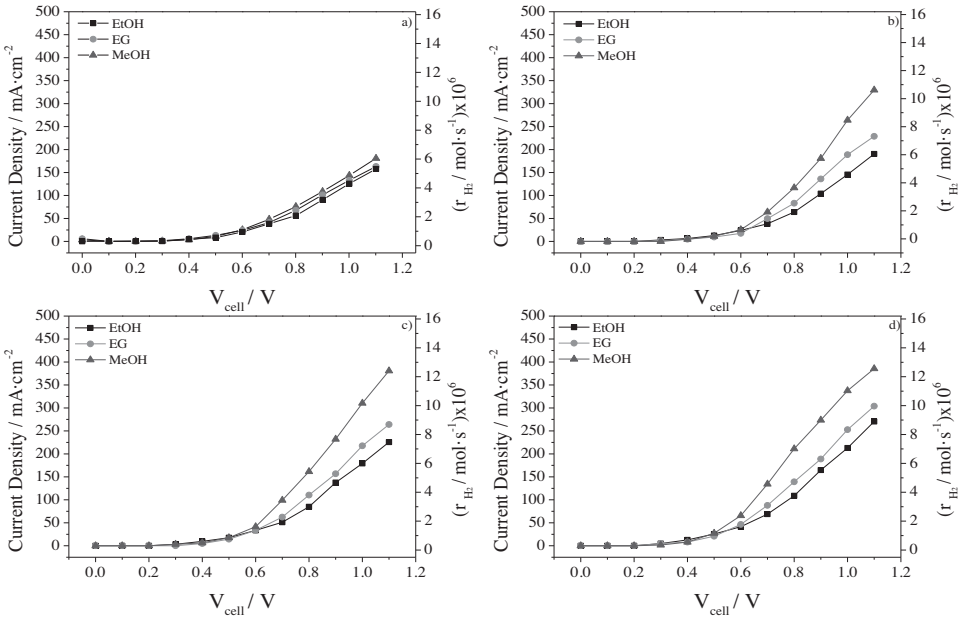

Fig. 4. Influence of the applied potential on the obtained current density for a 6 M alcohol/water solutions. (a) 60 °C; (b) 70 °C; (c) 80 °C; (d) 90 °C.

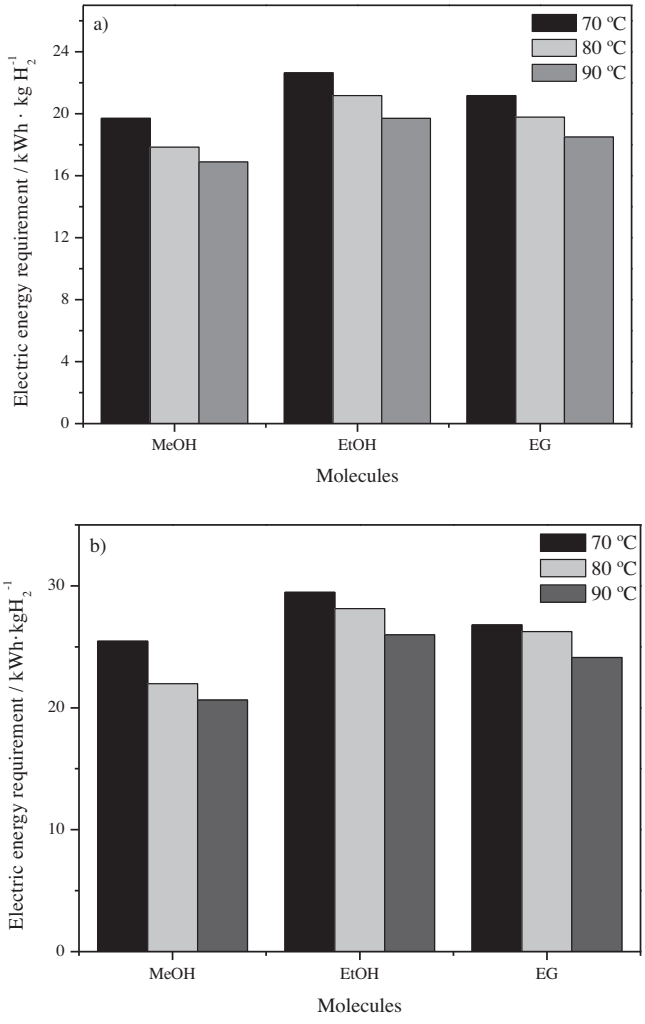

Fig. 5. Electrical energy consumption at different temperatures for different alcohol/water solutions. (a) 0.5 A (0.08 A cm^{-2}); (b) and 1.2 A (0.192 A cm^{-2}).

for a more precise economic evaluation, such as electrode area requirements (depending on selected current density) or cost of the feedstock. It can be also observed that the lowest energy investment was derived from the use of methanol/water solutions followed by ethylene glycol/water and ethanol/water solutions, respectively. In agreement with polarization curves, it can be attributed to the following electrocatalytic reaction rate order: methanol > ethylene glycol > ethanol that has been explained according to the combined effect between Pt and Sn. It seemed to promote C—C bond scission in the ethylene glycol molecule, which is comparable to the electrochemical results obtained with commercial Pt–Ru/C catalyst. The high catalytic activity of Pt_7–Sn_3/C can be associated with the presence of oxygen-containing species adsorbed on Sn atoms and a proper geometry of Pt and Sn sites on the catalyst surface. However, difference between the three molecules is not very important (below 10%) at fixed conditions ([organic molecule]:6 M, 70–90 °C, current: 0.5 and 1.2 A). Therefore, electrochemical reforming over synthesized Pt_7–Sn_3/C anodic catalyst is a suitable technique for H_2 production from biomass-derived alcohol molecules, which typically contain ethanol, methanol and ethylene glycol, as explored in this work. Furthermore, in all cases the electrical energy requirement was below 30 kWh $kg_{H_2}^{-1}$, around 60% of the energy demand in commercial water electrolyzer stack (50 kWh $kg_{H_2}^{-1}$).

Finally, in order to check the stability of catalyst Pt_7Sn_3/C for practical application purposes, a mild-time electrochemical reforming experiment was carried out. The experiment was run for 10 h at 80 °C under constant current density (0.08 A cm^{-2}, 0.5 A), by feeding a 6 M ethanol solution to the anode (1 ml/min). As shown in Fig. 6, an important increase of potential was observed during the first 3 h of operation. However, after that period, the system seemed to attain a steady-state voltage value that led to a stable operation for at least another 7 h. A similar behavior has been observed by Lobato et al. [46] in a long working polybenzimidazole (PBI)-based direct ethanol fuel cell and in previous works of electrochemical reforming of ethanol [11] and bioethanol [13] with Pt–Ru/C anodic catalyst. On this kind of systems, the observed deactivation with time on stream can be related to either higher swelling degree of the polymer membrane [47] or poisoning of the anodic catalyst [48] at high concentrated alcohol solutions. A recent work of our group

Table 3
Comparison of energy consumption for electrochemical reforming of ethanol at 0.5 A before and after deactivation. Kg^{-1}

	Anodic catalyst composition	Anodic catalyst loading (mg/cm^2)	V (V)	I (A)	$r\ H_2$ (mol/s)	Power (kW)	Energy requirement ($kW\,h\,Kg_{H_2}{}^{-1}$)	Yield (kg H_2 ($kW\,h\,kg_{cat}$)$^{-1}$)	Yield (kg H_2 ($kW\,h\,kg_{Pt}$)$^{-1}$)	Ref.
Fresh Pt_7–Sn_3/C	20% (Pt_7Sn_3)/C	1.5	0.77	0.5	2.59	3.85×10^{-4}	20.64	5167.96	36913.99	Present
Deactivated Pt_7–Sn_3/C			1.00		×	5.00×10^{-4}	26.81	3978.61	28418.68	work
Fresh commercialPt–Ru/C	60% (Pt_4Ru_2)/C	3	0.70		10^{-6}	3.5×10^{-4}	18.76	2842.93	11845.53	[11]

Table 4
GC-analysis of the cathodic and anodic outer streams of the PEM electrochemical reforming reactor during the stability test experiment.

	Sample	Product analysis (mol.%)							
		Acetaldehyde	Ethanol	Acetic acid	Acetone	Others	Hydrogen	CO	CO_2
Anodic chamber	Initial (liquid)	Traces	99.960	–	0.030	<0.010	–		
	After 10 h (liquid)	7.800	91.770	0.002	0.420	0.008	–		
	After 10 h (gas)	18.011	21.336	0.001	0.426	0.007	0.004	0.055	60.160
Cathodic chamber	After 10 h (gas)	–					99.938	0.008	0.054

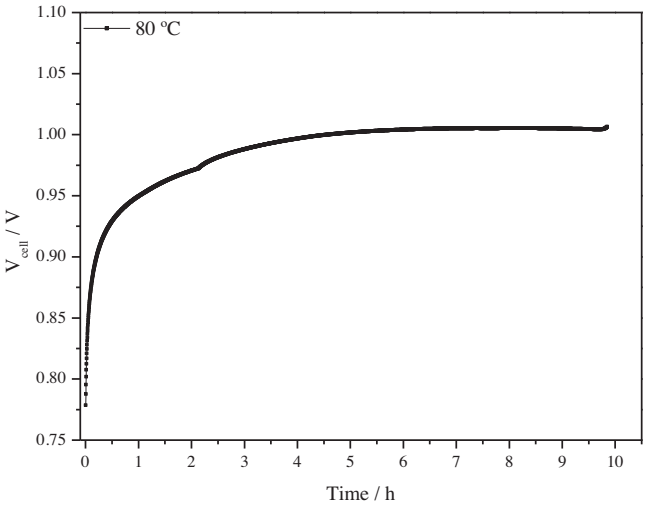

Fig. 6. Stability test: potential variation vs. time on stream at fixed applied current. Conditions: ethanol concentration: 6 M, temperature: 80 °C, current 0.5 A.

has demonstrated by AC impedance spectroscopy that the main origin of deactivation during electrochemical reforming of bioethanol on Pt–Ru/C anodic catalyst is the adsorption of reaction intermediates and products (e.g., acetaldehyde, acetic acid...), which led to an increase in the polarization resistance of the anode. From these results, stability of the proposed system was proved, demonstrating its feasibility for possible practical application.

Table 3 reports a comparison between the energy estimation for H_2 production ascribed to the proposed Pt_7–Sn_3/C anodic catalyst (both at the beginning and after 10 h of operation) and the commercial Pt–Ru-based one. An increase of working voltage for the production of a fixed amount of H_2 leads to an increase of the electrical energy demand of 6 $kWh\,kg_{H_2}{}^{-1}$ for the selected working conditions. Then, a final value close to 27 $kWh\,kg_{H_2}{}^{-1}$ was attained on the deactivated Pt_7–Sn_3/C catalyst under steady-state conditions. A recent work of Chen et al. [14] reported a lower energy consumption value (18.49 $kWh\,kg_{H_2}{}^{-1}$) for electrochemical reforming of ethanol on the fresh state of Pd/TiO_2 nanotubes in alkaline media. However, it should be mentioned that in that work, 9.9 Kg of NaOH were required for the production of 1 Kg of hydrogen [14]. In our present configuration, based on PEM, no additional reactants are requested and the amount of energy needed for the steady-state production of hydrogen, even after deactivation, is still much lower than the energy requirement of commercial PEM water electrolyzers. In this sense, the US Department of Energy (DOE) has pointed out that the electrical energy input to the electrolyze stack should drop to 43 $kWh\,kg_{H_2}{}^{-1}$ by 2020 [49]. Even considering the DOE output energy for ethanol of 7.4 $kWh\,kg_{H_2}{}^{-1}$ [50], the required electrical energy for ethanol electrochemical reforming over Pt_7–Sn_3/C catalyst seems to be a competitive technology, specifically for H_2 production from biomass alcohol streams. Furthermore, it can be also noted (Table 3) that if catalyst (or Pt) requirements to produce 1 kg of pure hydrogen are also considered, the suggested system provides a higher yield than that based on the fresh commercial catalyst. However, it should be mentioned that this difference could be lower in case Pt–Ru/C catalyst loading was equivalent to that of the synthetized Pt_7–Sn_3/C. Higher catalyst loadings are found not to improve electrochemical active surface area. In addition to reduced energy and catalyst needs, the great cost savings derived from replacing Pt by Sn (10 times cheaper) make Pt_7–Sn_3/C a promising alternative for further investigations, process optimization and possible scale-up.

Regarding products analysis, Table 4 collects both gas and liquid outstream products from the anodic and cathodic sides of the PEM electrochemical reforming reactor during operation of the mild-term reaction experiment presented in Fig. 6. Ideal ethanol electroreforming process happen as described in Eqs. (4)–(6). However, in the anodic chamber other reactions may occur [41] such as:

ethanal diethylacetal that can be formed in a follow-on reaction by acid catalysis:

$$CH_3CHO + CH_3CH_2OH \rightleftharpoons CH_3CH(OCH_2CH_3)_2 + H_2O \quad (10)$$

oxidation to ethylacetate:

$$CH_3CH_2OH + H_2O \rightarrow CH_3COOH + 4H^+ + 4e^- \quad (11)$$

$$CH_3COOH + CH_3CH_2OH \rightleftharpoons CH_3COOCH_2CH_3 + H_2O \quad (12)$$

or in a more difficult extent, complete oxidation

$$CH_3CH_2OH + 3H_2O \rightarrow 2CO_2 + 12H^+ + 12e^- \quad (13)$$

It can be observed from Table 4 that liquid analysis of the anodic side of the PEM revealed acetaldehyde as the main electrooxidation product. Therefore, partial oxidation of ethanol to acetaldehyde (Eq. (4)) seems to be the preferential oxidation mechanism instead of oxidation of ethanol to acetic acid (Eq. (11)). In the gas phase of the anodic chamber, mainly ethanol and acetalde-

hyde were found due to evaporation of both compounds. As seen, a little amount of acetone was also formed, which could be due to aldol condensation of acetaldehyde [51,52]. In addition, although it is more difficult than in case of methanol, certain complete ethanol oxidation was achieved since a large amount of CO_2 was detected (due to discontinuous operation mode). With respect to the cathodic chamber of the PEM, it is worthy to remark that a high purity H_2 was obtained (99.938%) and only a few ppm of CO (80 ppm) and CO_2 (540 ppm) were detected. The presence of these carbon-based compounds is due to the partial permeability of these gases across the membrane from the anodic side, revealing further oxidation of part of acetaldehyde by adsorbed water, according to the bi-functional mechanism [20,43]. Moreover, adsorbed OH^- species on Sn atoms can preferentially oxidize adsorbed acetyl species (CH_3CO_{ads}) to CO and CO_2 instead to CH_3COOH (no detected in the GC FID-analysis). Therefore, as commented above, the formation of such intermediate oxidation products (CH_3CHO and CO) may be responsible of the partial deactivation of the system observed on Fig. 6. Finally, from results outlined in Table 4, an overall ethanol conversion of around 8% was estimated after 10 h of operation.

4. Conclusions

The following conclusions are obtained from this study:

- Modified polyol reduction method can be effectively used for the synthesis of active Pt_7–Sn_3/C anodic catalyst for selective hydrogen production through electro-oxidation of organic compounds from biomass resources (methanol, ethanol and ethylene glycol).
- Synthesized nanostructured Pt_7–Sn_3/C catalyst presents bi-phase structure that consists of face-centered cubic (fcc) Pt and amorphous SnO_x phases. XPS analysis revealed that the catalyst surface contains both metallic Pt and Sn, as well as oxides: PtO, $Pt(OH)_2$, PtO_2 and SnO_x. Furthermore, Pt_7–Sn_3/C shows small particle size of 4.5 nm and over a narrow size distribution.
- Electrochemical reforming of biomass-derived alcohols (methanol, ethanol, ethylene glycol) solutions over the proposed bimetallic Pt_7–Sn_3/C anodic (20 wt.% loading) catalyst led to the production of high purity hydrogen (99.938%) under the application of low polarizations (0.4–1.1 V) in a PEM electrolyzer.
- Pt_7–Sn_3/C seems to require similar energy consumptions than Pt–Ru/C but requires lower amounts of Pt in order to produce the same amount of hydrogen. As a result, the suggested system provides a higher yield than that based on the fresh commercial catalyst. It could be associated with a synergic effect between the facilitation of alcohol-oxidation via oxygen containing adsorbed species on Sn atoms and the suitable geometry of Pt and Sn on the catalyst surface that weakens the adsorption of CO and other intermediates. In addition, the great cost savings derived from replacing Pt by Sn make this catalyst a promising alternative for further investigations and possible scale-up.
- A stable electrocatalytic activity was proved during the mild-term electrochemical reforming experiments using ethanol as fuel, demonstrating that the suggested PEM electrolyzer is able to efficiently produce hydrogen with an electrical energy requirement around 60% lower than that of a commercial PEM water electrolyzer stack (50 kWh $kg_{H_2}^{-1}$).

Acknowledgments

Financial Support from the Spanish Ministerio de Ciencia e Innovación (CTQ2013-45030-R) is gratefully acknowledged.

References

[1] M. Momirlan, T.N. Veziroglu, Renew. Sustain. Energy Rev. 6 (2002) 141–179.
[2] A. Nieto-Márquez, D. Sánchez, A. Miranda-Dahdal, F. Dorado, A. De Lucas-Consuegra, J.L. Valverde, Chem. Eng. Process.: Process Intensif. 74 (2013) 14–18.
[3] H. Takenaka, E. Torikai, Y. Kawami, N. Wakabayashi, Int. J. Hydrogen Energy 7 (1982) 397–403.
[4] Summary of electrolytic hydrogen production, In: N.R.E. Laboratory (Ed.) USA Report NREL/MP, pp. 560–36734.
[5] T. Take, K. Tsurutani, M. Umeda, J. Power Sour. 164 (2007) 9–16.
[6] G. Sasikumar, A. Muthumeenal, S.S. Pethaiah, N. Nachiappan, R. Balaji, Int. J. Hydrogen Energy 33 (2008) 5905–5910.
[7] C.R. Cloutier, D.P. Wilkinson, Int. J. Hydrogen Energy 35 (2010) 3967–3984.
[8] Z. Hu, M. Wu, Z. Wei, S. Song, P.K. Shen, J. Power Sour. 166 (2007) 458–461.
[9] A.T. Marshall, R.G. Haverkamp, Int. J. Hydrogen Energy 33 (2008) 4649–4654.
[10] S. Kongjao, S. Damronglerd, M. Hunsom, J. Appl. Electrochem. 41 (2011) 215–222.
[11] A. Caravaca, F.M. Sapountzi, A. De Lucas-Consuegra, C. Molina-Mora, F. Dorado, J.L. Valverde, Int. J. Hydrogen Energy 37 (2012) 9504–9513.
[12] C. Lamy, T. Jaubert, S. Baranton, C. Coutanceau, J. Power Sour. 245 (2014) 927–936.
[13] A. Caravaca, A. De Lucas-Consuegra, A.B. Calcerrada, J. Lobato, J.L. Valverde, F. Dorado, Appl. Catal. B: Environ. 134–135 (2013) 302–309.
[14] Y.X. Chen, A. Lavacchi, H.A. Miller, M. Bevilacqua, J. Filippi, M. Innocenti, A. Marchionni, W. Oberhauser, L. Wang, F. Vizza, Nat. Commun. 5 (2014).
[15] A. De Lucas-Consuegra, A.B. Calcerrada, A.R. De La Osa, J.L. Valverde, Fuel Process. Technol. 127 (2014) 13–19.
[16] G. Rabenstein, V. Hacker, J. Power Sour. 185 (2008) 1293–1304.
[17] K.-W. Park, J.-H. Choi, B.-K. Kwon, S.-A. Lee, Y.-E. Sung, H.-Y. Ha, S.-A. Hong, H. Kim, A. Wieckowski, J. Phys. Chem. B 106 (2002) 1869–1877.
[18] A. Oliveira Neto, E.G. Franco, E. Aricó, M. Linardi, E.R. Gonzalez, J. Eur. Ceram. Soc. 23 (2003) 2987–2992.
[19] A.O. Neto, R.R. Dias, M.M. Tusi, M. Linardi, E.V. Spinacé, J. Power Sour. 166 (2007) 87–91.
[20] F. Vigier, C. Coutanceau, F. Hahn, E.M. Belgsir, C. Lamy, J. Electroanal. Chem. 563 (2004) 81–89.
[21] S.W. Xie, S. Chen, Z.Q. Liu, C.W. Xu, Int. J. Electrochem. Sci. 6 (2011) 882–888.
[22] J. De Paula, D. Nascimento, J.J. Linares, Chem. Eng. Trans. 41 (2014) 205–210.
[23] W. Zhou, Z. Zhou, S. Song, W. Li, G. Sun, P. Tsiakaras, Q. Xin, Appl. Catal. B: Environ. 46 (2003) 273–285.
[24] L. Jiang, G. Sun, S. Sun, J. Liu, S. Tang, H. Li, B. Zhou, Q. Xin, Electrochim. Acta 50 (2005) 5384–5389.
[25] S.C. Zignani, V. Baglio, J.J. Linares, G. Monforte, E.R. Gonzalez, A.S. Aricò, Electrochim. Acta 70 (2012) 255–265.
[26] E. Antolini, E.R. Gonzalez, Electrochim. Acta 56 (2010) 1–14.
[27] C. Lamy, S. Rousseau, E.M. Belgsir, C. Coutanceau, J.M. Léger, Electrochim. Acta 49 (2004) 3901–3908.
[28] E.R. Savinova, F. Hahn, N. Alonso-Vante, Surf. Sci. 603 (2009) 1892–1899.
[29] W.J. Zhou, S.Q. Song, W.Z. Li, Z.H. Zhou, G.Q. Sun, Q. Xin, S. Douvartzides, P. Tsiakaras, J. Power Sour. 140 (2005) 50–58.
[30] E. Baranova, T. Amir, P.J. Mercier, B. Patarachao, D. Wang, Y. Le Page, J. Appl. Electrochem. 40 (2010) 1767–1777.
[31] E.A. Baranova, M.A. Padilla, B. Halevi, T. Amir, K. Artyushkova, P. Atanassov, Electrochim. Acta 80 (2012) 377–382.
[32] E.A. Baranova, C. Bock, D. Ilin, D. Wang, B. MacDougall, Surf. Sci. 600 (2006) 3502–3511.
[33] C. Bock, C. Paquet, M. Couillard, G.A. Botton, B.R. MacDougall, J. Am. Chem. Soc. 126 (2004) 8028–8037.
[34] E.A. Baranova, K. Artyushkova, B. Halevi, T. Amir, U. Martinez, P. Atanassov, ECS Trans. 41 (2011) 1691–1700.
[35] E.A. Baranova, Y. Le Page, D. Ilin, C. Bock, B. MacDougall, P.H.J. Mercier, J. Alloys Compd. 471 (2009) 387–394.
[36] S. Weissmann, Metal and Alloys, Data Book Center for Diffraction Data JCPDS, Pennsylvania, 1981.
[37] K. Artyushkova, B. Halevi, M. Padilla, P. Atanassov, E.A. Baranova, J. Electrochem. Soc. 162 (2015) H345–H351.
[38] A. Oliveira Neto, R.R. Dias, V.A. Ribeiro, E.V. Spinacé, M. Linardi, Eclética Quím. 31 (2006) 81–88.
[39] A. Oliveira Neto, M.J. Giz, J. Perez, E.A. Ticianelli, E.R. Gonzalez, J. Electrochem. Soc. 149 (2002) A272–A279.
[40] F. Vigier, C. Coutanceau, A. Perrard, E.M. Belgsir, C. Lamy, J. Appl. Electrochem. 34 (2004) 439–446.
[41] J. Wang, S. Wasmus, R.F. Savinell, J. Electrochem. Soc. 142 (1995) 4218–4224.
[42] H. Yue, Y. Zhao, X. Ma, J. Gong, Chem. Soc. Rev. 41 (2012) 4218–4244.
[43] B.Z.W. Zhou, Z. Zhou, W. Li, S. Song, Z. Wei, G. Sun, Q. Xin, Nanotechnology in Catalysis, in: S.H. Bing Zhou, G.A. Somorjai (Eds.), Kluwer Academic/Plenum Publishers, 2004, pp. 183–200, chapter 9.
[44] L. Jiang, Z. Zhou, W. Li, W. Zhou, S. Song, H. Li, G. Sun, Q. Xin, Energy Fuels 18 (2004) 866–871.
[45] T.E. Shubina, M.T.M. Koper, Electrochim. Acta 47 (2002) 3621–3628.
[46] J. Lobato, P. Cañizares, M.A. Rodrigo, J.J. Linares, Fuel Cells 9 (2009) 597–604.
[47] J.A. Elliott, S. Hanna, A.M.S. Elliott, G.E. Cooley, Polymer 42 (2001) 2251–2253.

[48] S. Song, G. Wang, W. Zhou, X. Zhao, G. Sun, Q. Xin, S. Kontou, P. Tsiakaras, J. Power Sour. 140 (2005) 103–110.
[49] Development and demonstration Plan of the US Department of Energy, In: D.O. Energy (Ed.), Fuel Cell Technology Office Multi-Year Reserach, 2011.
[50] H. Shapouri, Energy Balance of the Corn-Ethanol Industry, In: USDA (Ed.), 2008.
[51] L. Mahdavian, Nat. Sci. 3 (2011) 471–477.
[52] T. Nishiguchi, T. Matsumoto, H. Kanai, K. Utani, Y. Matsumura, W.-J. Shen, S. Imamura, Appl. Catal. A: Gen. 279 (2005) 273–277.